

**LARGE SCALE VORTICES
IN THE MAGNETOSPHERIC BOUNDARY LAYER**

*Comunicación del Ciclo Ciencia y Desarrollo
efectuado por el Dr. F. T. Gratton, el Dr. L. Bilbao,
la Dra. G. Gnavi y el Dr. C. J. Farrugia,
acto organizado por el Instituto de Investigación y Desarrollo
de la Academia Nacional de Ciencias de Buenos Aires
el 27 de mayo de 2010*

FAUSTO TULLIO LIVIO GRATTON

Fausto T. L. Gratton (argentino naturalizado) es Licenciado y Doctor en Física de la *Universidad de Buenos Aires* (UBA). Es Investigador Superior del *Consejo Nacional de Investigaciones Científicas y Técnicas* (CONICET) con lugar de trabajo en el *Instituto de Física del Plasma* (CONICET – FCEyN/UBA). Fue co-fundador y director (hasta junio de 2009) de dicho Instituto (<http://www.lfp.uba.ar>).

Se ha especializado en física del plasma (gases ionizados). Ha publicado como primer autor o coautor alrededor de 170 trabajos en revistas internacionales, o actas de congresos internacionales con referato en plasmas espaciales, magnetohidrodinámica, fusión nuclear y teoría de plasmas –a menudo por invitación– y una docena de ensayos de epistemología e historia de la física.

Ha recibido numerosos subsidios para la investigación de CONICET, UBACYT, VITAE, OEA, entre otras instituciones. Actualmente trabaja en magnetohidrodinámica y física de la magnetosfera terrestre como director del proyecto 1122009 0100608 PIP 2010-2012 del CONICET y co-director del proyecto UBACYT X90/08.

Ha pronunciado más de un centenar de coloquios y conferencias en instituciones científicas de Europa, USA y América Latina. Mantiene una activa colaboración con investigadores del *Space Science Center*, University of New Hampshire, NH, USA y participó en el proyecto de la NASA, NAG 5-13116, 2003-2005. Entre las recientes conferencias por invitación sobre resultados de esta colaboración menciona: *The 2008 Huntsville Workshop: Physical Processes for Energy and Plasma Transport across Magnetic Boundaries*, October 26-31, 2008 Huntsville, AL, USA. *American Geophysical Union Fall Meeting: Magnetospheric Response to Solar Wind Discontinuities (SM07)*, 15-19 December 2008, San Francisco, USA. *10th. Brazilian Meeting on Plasma Physics*, 25-28 November 2009, Maresias, SP, Brazil. *Fluidos 2010*, XI Int. Meeting on Recent Advances in Fluid Physics and Applications, Colonia del Sacramento, Uruguay, 3-5 noviembre 2010.

Fue Profesor Titular de Física (dedicación exclusiva, por concurso) desde 1973 a 2004 en la *Facultad de Ciencias Exactas y Naturales* de la Universidad de Buenos Aires. Actualmente es Profesor Titular de Física (dedicación simple) de la *Facultad de Ciencias Fisico-matemáticas e Ingeniería*, de la Pontificia Universidad Católica Argentina (UCA, desde 2005). En la UCA es también miembro de la Comisión de Investigación del Consejo Superior y consultor del Consejo de Investigaciones del Rectorado.

A nivel universitario, en el país y en el exterior, ha dictado cursos de plasmas, fusión nuclear, mecánica de fluidos, mecánica estadística, electricidad y magnetismo. Ha dirigido once tesis de doctorado en física de la FCEyN/UBA y quince becarios de investigación.

Es Académico Titular de la *Academia Nacional de Ciencias de Buenos Aires* desde 2001. En la Academia preside la Sección de Ciencias Exactas y Naturales. Fue Subdirector hasta 2010 y es Director desde 2011 del *Instituto de Investigación y Desarrollo Amílcar Argüelles* de esa institución.

Es Miembro Consultor del *Consejo Argentino para las Relaciones Internacionales* en el Comité de Asuntos Nucleares Internacionales, desde 2007.

Ha sido miembro del directorio del CONICET en 1990-1991 y varias veces miembro de comisiones asesoras y junta de calificaciones de ese organismo. Durante varios años ha sido profesor invitado (a nivel de profesor titular) en la *Technische Universität* y la *Karl Franz Universität*, dos universidades estatales de la ciudad de Graz, Austria. En numerosas ocasiones fue investigador visitante en universidades e institutos científicos de EE.UU., Inglaterra, Italia, Brasil, Chile y Colombia. Fue nombrado representante por América Latina del *Comité de Científicos Italianos del Mundo* del Gobierno de la República de Italia, período 2002-2006.

LARGE SCALE VORTICES IN THE MAGNETOSPHERIC BOUNDARY LAYER

Dr. F. T. GRATTON^{1,3,4}

Dr. L. BILBAO¹

Dra. G. GNAVI¹

Dr. C. J. FARRUGIA²

Abstract

We report the results of increasing the speed of the magnetosheath plasma to supersonic and superAlfvénic levels on the dynamics of large vortices formed in the boundary layer of the terrestrial magnetopause. The study is based on computational magneto-fluid dynamics. The boundary layer model is designed with spacecraft data (Cluster mission) observed on December 7, 2000. The distinctive features of this configuration are *a*) very small magnetic shear across the boundary, and *b*) the physical activity concerns mainly the vorticity; the magnetic field is only fluted during the process, but it determines the direction of the vortex axis and other features. In addition, we analyze correlations of data to identify signatures of the Kelvin-Helmholtz instability, and the presence of a whirling plasma in the boundary layer. The new results extend an earlier investigation presented at this Academy (*Anales*, Vol. XL, 2007) along two lines: *i*) the magnetosheath flow increase up to supersonic and superAlfvénic speeds on vortex simulations; *ii*) the analysis of data correlations that may disclose the existence of a vortical boundary layer. The purpose is to contribute to the elucidation of factors that govern the plasma entry into the magnetosphere during periods of northward interplanetary magnetic field.

¹ *Grupo de Plasmas Espaciales*, Instituto de Física del Plasma (CONICET-UBA), Ciudad Universitaria, Pab. 1, Buenos Aires CP1428, Argentina.

² *Space Science Center*, Earth, Ocean, and Space Institute, University of New Hampshire, Durham, NH, 03824, USA.

³ *Departamento de Física*, Facultad de Ciencias Fisicomatématicas e Ingeniería, Pontificia Universidad Católica Argentina, Buenos Aires, Argentina.

⁴ *e-mail*: fgratton@arnet.com.ar, fgratton@infip.org

Resumen

Presentamos resultados de la dinámica de grandes vórtices formados en la capa límite de la magnetopausa terrestre obtenidos aumentando la velocidad del plasma de la magnetovaina al régimen supersónico y super-Alfvénico. El estudio se basa en la magneto-fluidodinámica computacional. El modelo de capa límite se construye con datos de satélite (misión Cluster) observados el 7 de diciembre de 2000. Las características distintivas de esta configuración son i) muy pequeña cizalla magnética a través de la frontera y ii) la física involucra principalmente la vorticidad; el campo magnético solo es “aflautado” por el proceso, pero determina la dirección del eje de los torbellinos y otras propiedades. Los nuevos resultados amplían una precedente investigación presentada a esta Academia (*Anales*, Vol. XL, 2007) en dos direcciones: *i*) el aumento de la velocidad de la magnetovaina en las simulaciones numéricas a velocidades supersónicas y superAlfvénicas; *ii*) el análisis de correlaciones de datos que pueden poner en evidencia la presencia de torbellinos en la capa límite. El objetivo es contribuir a la comprensión de los factores que gobiernan la entrada de plasma a la magnetosfera durante períodos de campo magnético interplanetario norte.

1. Introduction

The stage of this work is the terrestrial magnetopause (MP). We focus attention on the boundary layer (BL) at the low latitude magnetosphere flanks. The paper deals with the computational magnetohydrodynamics (MHD) of large vortices. These often form at the BL, and appear more frequently when the interplanetary magnetic field (IMF) shows a significant north component. In addition, we discuss a matter of considerable interest in view of the scarcity of *in situ* observations. Can records of a single spacecraft, which crosses the BL during the transit of quasi-periodic perturbations, pass a judgment of vortex detection?

The paper is a development of an investigation presented earlier at this Academy [1] (then extensively in [2]) along two directions: *i*) the effect on vortex simulations of increasing the magnetosheath flow up to supersonic and superAlfvénic speeds, and *ii*) the correlations of experimental data that may disclose the presence of vortices in the BL.

A cold, dense, magnetized plasma flows around the magnetosphere, gathering speed as it progresses tailward. A general descrip-

tion of magnetic fields and flows can be found, for instance, in [3]. A puzzling phenomenon is a cause of concern in magnetospheric physics. Increasingly, attention has been directed to the presence of magnetosheath plasma deep inside the Earth’s plasma sheet when the IMF stays northward for long spells. This plasma is relatively (with respect to ordinary values in the same regions) cold, dense, and stagnant (for example, $T \cong 1 \text{keV}$, $N \sim 1 \text{cm}^{-3}$). See, among other references, [4, 5, 6, 7]. The phenomenon is known as the cold dense plasma sheath (CDPS).

The difficulty is to explain how did this CDPS get there. The presence in the Earth’s geomagnetic tail of plasma with properties similar to that of the adjoining magnetosheath makes the flanks a likely entry locale. Indeed, flank entry has often been advocated to explain episodes of CDPS (e.g., [8]). The data records are also well correlated with periods of northward IMF. Hence, the problem is the mechanism of mass entry from solar wind into magnetosphere during northward IMF periods [5, 8].

Among the processes that have been suggested, we consider the velocity shear instability (Kelvin-Helmholtz instability, KH) in the non-linear stage, when rolled-up vortices that entrain magnetosheath material, and broaden the BL, are formed. In the last decade this hypothesis has gained strength and support by several investigations (see, among other references [1, 2, 9, 10, 11, 12, 13, 14, 15, 16, 17, 18, 19, 20, 21] and the literature quoted therein). Inside large vortices, the close mingling of magnetosheath with magnetosphere plasma favors the enhancement of particle diffusion at the microscopic scale.

In this investigation we study a KH scenario based on the plasma and magnetic field configuration recorded by the Cluster mission during an event of December 7, 2001. In the context of the current literature, the distinctive features of our work, are: i) a very small magnetic shear across the boundary, and ii) a dynamics that concerns mainly the vorticity. The process only flutes the magnetic field, although the latter determines the direction of the vortex axis [1, 2, 23, 24]. In another aspect, our simulations differ from other investigations: we use a local MP model with two free boundaries. The perturbations are free, not anchored, also in the direction normal to the flow (in the sense of the geomagnetic field).

An intrinsic difficulty of the CDPS issue is the dearth of “*in situ*” records. The boundary layer is not observable from afar with other methods, as it happens with several astrophysical systems. For the

greatest part one spacecraft alone, if at all, is crossing the MP at interesting times. Moreover, during a spacecraft crossing of the BL, it would be desirable to have the support of another in the neighbourhood to know the state of the magnetosheath at the same time, but this is a rare occurrence. Hence, the interest to have criteria to identify vortices with data from one spacecraft alone.

Many aspects of the connection of KH with CDPS remain obscure: several factors must be taken into account. The strength and orientation of the magnetosheath's magnetic field. Both magnetic and velocity shears, and the density gradient across the MP. The scale lengths of the magnetic and velocity transitions (which may be different (e.g., [22, 26]). The magnetosheath flow speed and the influence of supersonic flows (where compressibility, a stabilizing agent, comes into play). The physical conditions at the boundary, and the distance from the subsolar point. Some of these elements have been considered by members of our team, and by coworkers in recent studies [1, 2, 20, 21, 23, 24, 25, 26, 27].

After this introduction, a concise information about December 7, 2000 (our reference event), and the computational method is found in section 2. Elements of the mentioned event are incorporated in the numerical studies. Section 3 presents the main numerical results, and their dependence on the sonic and Alfvén Mach numbers. The evolution of BL strata with different temperature and density lead to section 4, which deals with correlations of December 7, 2000 data, and their interpretation. A summary is in section 5.

2. Brief notes on December 7, 2000 and the computational code

2.1 The reference event. Records from a crossing of the MP by Cluster on December 7, 2000 suggest the boundary layer models, the particular disposition of velocity and magnetic fields, the density and temperature stratification, employed in this paper. The phenomenology of this event and the associated theoretical and computational models are explained in detail in [1, 2, 23, 24, 26]. Only a minimal description is reported here to allow the reader to continue without a search of the references.

The period of interest is from 13:55 - 14:28 UT. Figure 1 shows plasma data from Cluster 3 while crossing the BL. The plot shows GSM (geocentric solar magnetospheric) velocity components, density, and temperature, versus time, UT, in decimal hours. The three lines

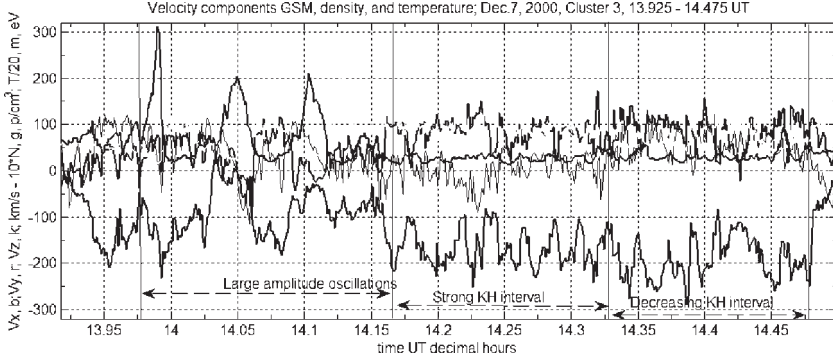


Figure 1. Data recorded by Cluster 3 on December 7, 2000. GSM velocity components versus time, UT in decimal hours. The three lower lines are for the velocity components, V_x deep black, V_y black, and V_z light black, km/s. Two upper lines are for particle density N (scale: $N \times 10 \text{ cm}^{-3}$) light gray, and temperature T (scale: $T/20 \text{ eV}$) light black.

closer to the bottom are for the velocity components, V_x deep black, V_y black, and V_z light black, km/s. The two upper lines are for particle density N (scale: $N \times 10 \text{ cm}^{-3}$) light gray, and temperature T (scale: $T/20 \text{ eV}$) dark gray. As can be seen, the time interval is divided in three parts that show intense BL activity. The time lapses are associated with changes of the IMF clock angle [23, 24], attested by the ACE spacecraft in the solar wind.

The first lapse, 13:58 - 14:10 UT corresponds to large amplitude boundary layer oscillations (with a period of about 3 min; 0.050 decimal hours) caused by the impact of a strong solar wind discontinuity onto the MP. The large excursions of the MP are used to obtain an estimate of the speed of the tailward flow in the adjacent magnetosheath, and to gauge the intensity and the change of direction of the magnetic field across the BL, from the magnetospheric inner edge to the magnetosheath [23, 24]. The survey reveals a MP configuration with a very small magnetic shear, favorable to the KH instability, and an external flow still subsonic and subAlfvénic.

The following two periods (with small magnetic shear across the BL) lasting from 14:10 - 14:28 are characterized by quasi-periodic oscillations with a shorter period, 79 s (0.0219 decimal hours). These are strong perturbations of all vector and scalar fields, with intensities decreasing during the third part of the event, from 14:20 to 14:28. After this, a change of the IMF clock angle determines mag-

netic conditions unfavorable to the KH instability, and in fact the former boundary layer activity observed by Cluster 3 extinguishes after 14:28 UT.

2.2 LES and computational code. We base our large eddy simulations (LES) on non-dissipative, compressible, MHD equations in 3D and time. A computational program, developed for complex magneto-fluid dynamics problems of plasma physics [28, 29, 30], was adapted for the present task. The in-house code starts from the integral conservative form of the MHD equations, and employs a *finite volume, Lagrangian-Eulerian* technique. The set of equations and a succinct information of the code’s features can be found in *Anales* of this Academy [1], or in reference [2]. More technical details are in [31, 32].

2.3 Initial and boundary conditions. Due to the very small magnetic shear, the MHD theory of the Kelvin-Helmholtz instability predicts significant growth rates for flute modes that have the most favorable angle between the \mathbf{k} – vector and the direction of the bulk flow at $\varphi=32^\circ$ [23, 24]. Modes with deviations of \mathbf{k} by 10 – 15 degrees from this orientation do not grow. The precise growth rate values depend on the averaged steady state model of the BL employed. A local piece of the BL is represented by a planar model. We assume hyperbolic tangent functions to connect continuously the vector and scalar fields (magnetic and velocity fields, density, and temperature) of the outer (magnetosheath) side with those of the inner (magnetospheric) edge.

The same configuration is used as the initial state for the LES, adding as a starter one perturbation mode to the velocity field only, with amplitudes about 5% of the magnetosheath speed. The computational results are presented in 3D boxes, with the X -axis pointing tailward, aligned with the magnetosheath flow. The Y -axis is normal to the local MP surface (a tangent plane), and points inward across the BL. The Z -axis completes a right-hand Cartesian triad (in this case, roughly a north direction). Thus, relative to the BL flow direction, X is streamwise, Y is transverse (across the flow, pointing into the magnetosphere), and Z is spanwise.

During the numerical simulation, the scalar and vector fields at the outer and inner limits of the BL are fixed at constant values as boundary conditions. In computational fluid dynamics, a *temporal* boundary layer has periodic conditions in the main flow direction (on the box sides’ normal to the X -axis). The LES of this paper are all of the temporal kind. A difference of our LES with respect to other simulation studies, is that we assume periodicity conditions also

along the Z-axis, so that perturbations may travel freely in a direction that points in the sense of the geomagnetic field.

Distances along the three axes are in units of the Earth radius (R_E). Note that for LES we chose the positive X-axis in a direction contrary to the GSM x -axis orientation used in Fig.1 and in the correlation analysis of section 4.

3. Numerical simulations: the increase of magnetosheath flow to supersonic and super-Alfvénic speeds

We compute the non-linear evolution of the KH instability with local BL models that portrait features observed during the Cluster crossing of December 7, 2000 [23, 24]. To investigate the influence of supersonic and superAlfvénic flow regimes on the boundary layer, we then extend the LES to higher magnetosheath speeds, preserving the same boundary values of magnetic field, temperature, and density. The computer runs are identified by numbers, like C42 that stand for case 42; the number originates from the book-keeping of the physical parameters of particular simulation runs, within a large size directory of numerical experiments. The results of only a few computer runs are reported here, and some of their properties are summarized in Table 1. The case number is in the first column, the second indicates the initial mode wavelengths that fits in the computing box. The third column gives the magnetosheath speed, V_l , in km/s, and

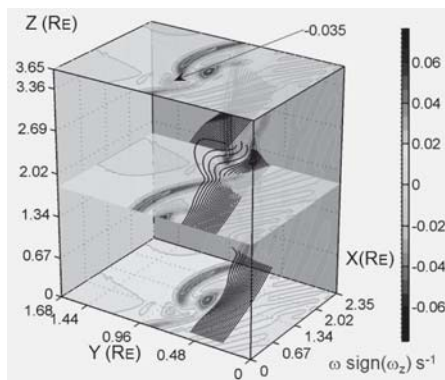


Figure 2. LES results for C42 at $t=132$ s, vorticity contours intensity with gray scale, and a set of (black) streamlines.

Table 1. Properties of the simulation cases

Case	wavelengths	V ₁ (km/s)	M	M _A	×
C42	λ	139	0.40	0.68	1
C62	3λ	278	0.80	1.36	2
C50	λ	420	1.21	2.05	3
C57	2λ	556	1.60	2.72	4

the last column indicates the increased speed factor with respect to the reference case C42. The fourth and fifth columns give the sonic, and Alfvén Mach numbers, respectively.

3.1 3-D flow complexity and counterrotating vorticity kernels.

Figure 2, shows the vorticity $\boldsymbol{\omega}=\text{curl}(\mathbf{V})$ for run C42, at $t=132$ s after the start, launched with one perturbation wavelength fitted into the box, and with the estimated magnetosheath speed for the December 7, 2000 event. Vorticity is represented by the absolute value $\omega=|\boldsymbol{\omega}|$, to which the sign of the Z component is associated with the formula $\Omega=\omega\times\text{sign}(\omega_z)$ s⁻¹. This is because ω_z is the main component that determines the orientation of the vorticity vector. Vorticity contours for Ω are shaded with gray scale. The perturbation wavevector is set initially at 32° with respect to the X -axis. Only one wavelength fits into the computing box (lengths are in Earth radii, R_E); the Y -axis scale length is twice that of the X, Z -axis to facilitate the view of the MP evolution.

The sonic and Alfvén Mach numbers are $M=0.40$ and $M_A=0.68$, respectively, evaluated on the magnetosheath side. The scenario is moderately subsonic and subAlfvénic. Compressibility effects are present but are not strong. The shape of the magnetic field is not appreciably changed because of the quasi-flute arrangement of the fastest growing mode. Nonetheless it is a dominant element, and influences the non linear evolution fixing the orientation of the vortex structures.

The initial vorticity layer has only positive Ω values. However, the non linear evolution not only intensifies Ω but generates also negative vorticity. Figure 2 shows the evolution of the vorticity layer at roughly $\frac{3}{4}$ of the turnover time for a vortex. Note the concentration of positive vorticity in a vortex core, with intensity amplified by 3D stretching, and the strained vorticity layer. Two negative vorticity patches have also developed, and are visible at positions of large strain of the shear layer, one closely associated with the positive vortex core. A set of streamlines, launched from positions near the

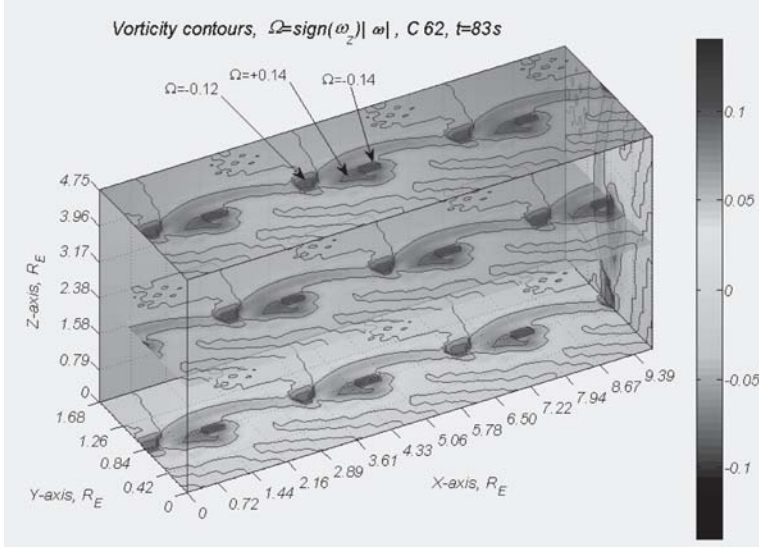


Figure 3. Vorticity contours for C62 at $t=83$ s. The magnetosheath speed is twice that corresponding to C42, and the computing box accepts three wavelengths.

magnetosheath side of the BL, are also shown. The flow is still laminar but is becoming increasingly 3D at this stage, and counterrotating vorticity cores develop.

We examined the presence of kinetic helicity with contour plots of kinetic helicity density $\mathbf{V} \cdot \boldsymbol{\omega}$ (not shown). In a BL with parallel shear flow $\mathbf{V} \cdot \boldsymbol{\omega}$ is initially zero, but as the vorticity layer suffers large deformations and large vortices are generated, kinetic helicities of both signs arise.

In Figure 3, that shows vorticity contours for C62 (with a gray scale) at $t=83$ s, the magnetosheath speed is 278 km/s, two times larger than the previous case C42. The magnetosheath flow is still subsonic $M=0.80$, albeit not by a wide margin, and is superAlfvénic $M_A=1.36$. The computing box elongated over the X-axis contains three wavelengths of the initial velocity perturbation. The plot shows the intensification of a row of positive vortices, and their pairing with negative vorticity centers, which are places strongly bent out of shape by the rolling over of the vortex sheet. The vorticity in the cores is many times larger than the initial, unperturbed, BL value.

The Mach numbers, sonic M and Alfvén M_A , of the runs characterize the external magnetosheath flow. Since at the inner edge of

the boundary layer the magnetosphere velocity is approximately zero, the physical state of motion inside the BL is governed by smaller values of the Mach parameters (if the magnetic field strength remains comparable to the magnetosheath value, as in this case). This is due not only to the decreasing average velocity in the BL, but also to the increase of temperature and the diminution of density, as we approach the magnetosphere side. Therefore, larger Mach numbers influence the physics of the BL only in runs with high speed, like cases C50 and C57.

We examined the process of coupling of vorticity centers of opposite signs at higher speed. In run C50 the magnetosheath speed is 420 km/s (increased three times from C42). The external flow is now supersonic, and superAlfvénic, $M=1.210$, $M_A=2.053$. The warping of the vorticity sheet and the rise of intense vortex cores are accelerated, these structures appear earlier. The pairing of large positive and negative vorticity concentrations in small regions is again present with intensified values. At $t=92.5$ s, a close pair of vorticity kernels have $\Omega=0.19$ and $\Omega=-0.14$ s⁻¹ (figure not shown). The vortex core is always aligned with the magnetic field direction, as illustrated further on.

3.2 Compressive effects. We now turn the attention to the effects of compressibility. Consider the reference configuration C42. Figure 4, left panel, shows vorticity contours on two sides, the bottom $Z=0$, and the backside $X=2.35 R_E$, of the computing box, and a set of

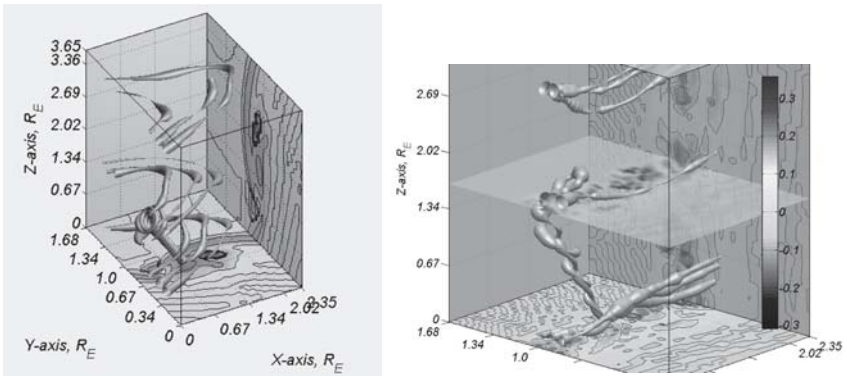


Figure 4. Left panel. Vorticity contours on $Z=0$, and $X=2.35 R_E$ with stream-tubes, C42, $t=132$ s. The tube section is proportional to $\text{div}(\mathbf{V})$. **Figure 4.** Right panel. Higher speed, close-up view of vorticity contours and stream-tubes, C50, $t=300$.

stream-tubes for $t=132s$. The tubes are similar to streamlines but with a finite section proportional to $\text{div}(\mathbf{V})$. The stream-tubes are launched at three different heights Z from the plane $X=0$ (the view is from a reference system moving tailward at half the magnetosheath speed). The tube section is normalized with the initial value at $X=0$, and the growth or diminution depends on the local value of $\text{div}(\mathbf{V})$. Therefore, the tube section reveals the relative rate of change of density with time, at each place along the tube. Stated with a formula, $\text{div}(\mathbf{V}) = - (1/\rho) (d\rho/dt)$, where the time derivative is computed by moving along with the flow (i.e, a Lagrangian quantity). Stream-tubes depict graphically the presence of compressibility effects.

The figure shows that the boundary layer is, in fact, subject to compressive activity, evidenced by the significant changes of tube sections. Thus, even at a subsonic magnetosheath speed, $M=0.40$ for case C42, the rolling-over dynamics, and the 3-D stretching, produce important compressive action in the boundary layer. However, when we examine the stream-tube captured, so to speak, by the vortex, which exhibits a swirling pattern, we note that the tube section remains constant as it coils around the vortex axis. We have examined for subsonic magnetosheath flows several other cases, and different times (omitted here for brevity). The pattern of compressibility effects is qualitatively similar to that displayed in Fig. 4, left. For subsonic flows, compressibility effects in the BL during the rollover are significant, but do not appear to affect the vortex core.

To contrast, Fig. 4, right panel illustrates results of C50 at $t=300s$ to emphasize differences. The speed of the outer flow is increased three times, 420 km/s, and the magnetosheath is supersonic, and superAlfvénic, $M=1.21$, $M_A=2.05$. With the same format as Fig. 4 left, the plot shows a close-up of stream-tubes. We observe inside the BL, as before, significant Lagrangian changes of density in action. However, now we note changes of the tube section of the stream-tube that coils around a vortex. At the magnetosheath speed level of C50, compressibility has influence also on vortex kernels dynamics.

3.3 Magnetic field. The magnetic field lines remain straight in all the cases examined. This is due to the small magnetic shear of the field configuration studied here. The fastest growing mode does not bend the magnetic field lines, the perturbations are flute-like, and maintain a flute pattern in the non linear phase. As time goes by, a slight swaying of the magnetic lines can be observed, similar to a wheat field undulating under a light breeze.

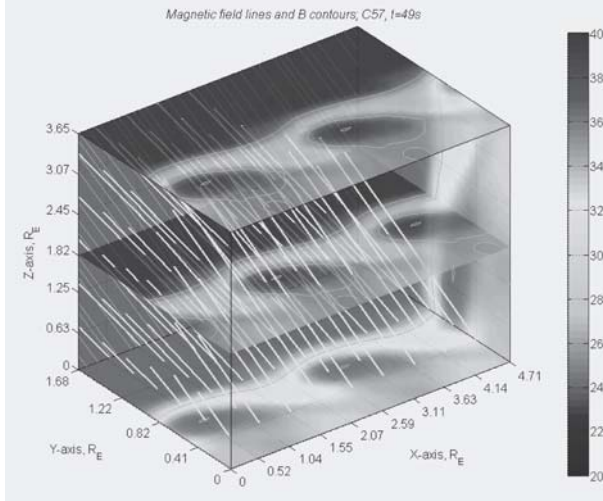


Figure 5. C57, B contours (absolute value of \mathbf{B}) with a gray scale, and magnetic field lines (white segments) $t=49s$.

Nevertheless, the presence of magnetic field is important as it determines the direction of the vortex axis. It also inhibits the development of streamwise vorticity, which is a common feature of ordinary fluid mixing layers. These are the so-called *hairpin* vortices (also known as longitudinal vortices) of the fluid dynamic literature, e.g., [33].

We examined streamwise vorticity with stream-ribbons. A stream-ribbon is defined like a streamline, with the line replaced by a ribbon of a given width. When there is vorticity along a streamline, the ribbon appears twisted in agreement with the projection of the angular velocity on the line direction. The twist of a stream-ribbons is proportional to $|\text{curl}(\mathbf{v})|$. However, the ribbons do not exhibit any worth noting degree of twist, including the ribbons that coil-up around a vortex kernel (figure not shown). We have examined several runs always with negative results, and came to the conclusion that streamwise vortices are absent in our LES. We conjecture that the presence of magnetic field is a hindrance for a process that occurs in ordinary fluids.

Magnetic pressure does not play any noticeable role in the equilibrium of the vortex core in subsonic runs (like C42 and C62). However, in supersonic runs like C57, $M=1.60$ (fourfold velocity increase) the kernel of largest vorticity becomes also a region of higher mag-

netic strength. The effect is illustrated in Fig. 5 which shows contours of absolute value of the magnetic field, with a gray scale, and a set of magnetic field lines (white) for $t=49s$. An increase of magnetic field strength in correspondence with vortex loci appears, a feature absent in LES at lower speeds.

3.4 Pairing and decrease of spatial periodicity. We consider now the pattern of vorticity contours for C57, the case of greatest speed studied. In Figure 6 the left panel is for $t=49s$, (the same time of Fig. 5) and shows the splitting of the vorticity sheet, and the presence of counter-rotating centers. The right panel of Figure 6 is for $t=99s$, where the pairing of split vortex cores, and the coupling of opposite rotation centers, can be observed. Some stream lines are also included in both panels. The LES reveals a doubling of the positive vorticity kernels in the box. A spacecraft in the boundary layer, therefore, should encounter vortices with a twofold increased frequency

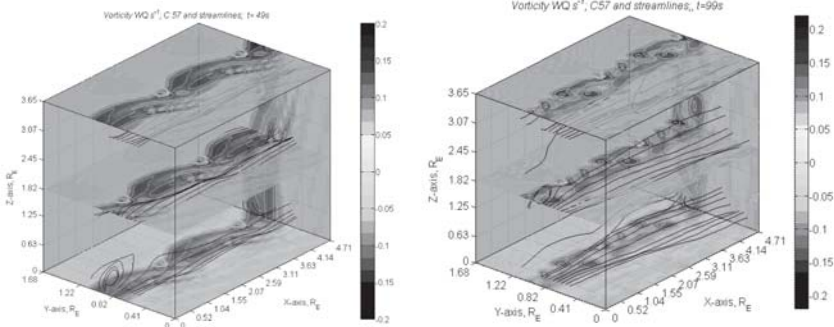


Figure 6. Change of periodicity by pairing. C57 vorticity and streamlines; the left panel is for $t=49s$, the right panel for $t=99s$.

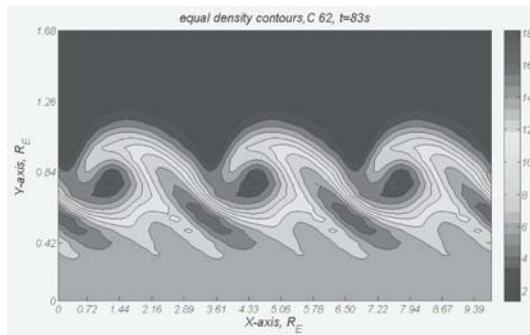


Figure 7. C62, isodensity contours at constant Z, N with a gray scale; $t=83s$.

with respect to the original perturbation. The modification of the period is produced by two kind of vorticity pairings, a positive - negative association, and the subsequent coupling of the previously associated pairs.

3.5 Density and temperature. The importance of temperature and density changes in the vortex cores is evident already at subsonic speeds. For the reference case C42, $t=180s$ (\sim one roll-over time) the plasma in the vortex centers is hotter ~ 3 times T_i (magnetosphere temperature), and more tenuous $\sim 1/3 N_i$ (magnetosphere particle density) than that of the adjacent magnetosphere [2]. We now consider the mixing of tenuous and hot (close to magnetosphere values) with dense and cold (near to magnetosheath levels) plasma.

Details of successive alternations of cold-dense and hot-tenuous portions of matter in the boundary layer can be appreciated in the following figures. The computer run is C62, with $V_1=278\text{km/s}$, $M=0.80$ $M_A=1.36$ (a twofold increase of speed with respect to C42). We plot equal density contours on planar slices at a fixed Z height. Fig 7 shows isodensity contours at $t=83$ s. The roll-over is evident, and it is also plain that the density pattern passing over a stationary spacecraft, as the plasma flows downstream, should leave a record of alternate density peaks and valleys, with peculiar shapes that depend on the observation point in the BL, and the time evolution of the vortical structures.

Similarly Fig.8 depicts equal temperature contours at a fixed Z plane, at $t= 105$ s. The alternation of high and low temperatures correlates well with the series of tenuous and dense plasma parts, so

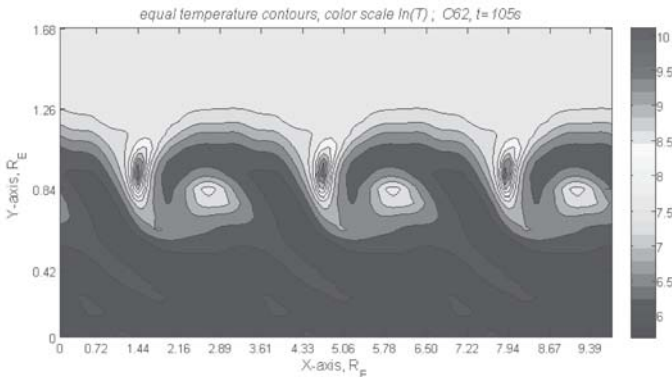


Figure 8. C62, equal temperature contours with a gray scale proportional to $\ln(T)$, at constant Z for $t=105s$.

that peaks and valleys are always associated in pairs of hot-tenuous and cold-dense sectors. The temperature of C62, at $t=105$ s, is very large in coincidence with positive vortex kernels, so that the gray scale of the plot is set with $\ln(T)$. The ratio of the hot spot to the magnetosphere temperature is in the 7 – 8 range.

Therefore, ideal MHD predicts the build-up of vortex cores that are also hot spots. It remains to be confirmed, by more elaborated dissipative MHD computations, the actual extent of the temperature rise predicted in vortex kernels. In any case, our LES indicate that the trend is there, and it poses a challenge to the ingenuity of the experimentalists to find out whether a significant temperature increment, concentrated in small places of the boundary layer, can be detected by spacecraft instruments.

4. Scatter plots of December 7, 2000 data and their significance

As can be seen in Fig.1, during the KH interval (14:10-14:28 UT) a principal part of the motion takes place in the x, y GSM plane. We therefore associate the X, Y , plane of the LES with this plane. The average of measured velocity over the period is $V_{av} = (-176.7, 85.1, 28.8)$ km/s. Note that, V_{yav} , the average of V_y data is not zero, because of the flaring of the magnetopause (the increasing span of the magnetosphere in the anti-sunward direction) at the position of Cluster 3, which estimated from the V_{yav}/V_{xav} ratio is about 26° (where V_{xav} is the corresponding V_x average). Thus, the actual y -axis is not normal to the MP, while the simulations assume that Y is normal to a MP model. In the following we work mainly with the x, y velocity components relative to the average, $U_x = V_x - V_{xav}$, $U_y = V_y - V_{yav}$. Hence, we consider the data from a tailward moving frame, with the y -flaring effect subtracted. We analyze scatter plots of December 7, 2000, Cluster 3 plasma data to find vortex signatures, i.e., to recognize patterns that herald the presence of whirling matter in the BL. The analysis is on a line similar to [18].

Figure 9 is a scatter plot where the x velocity component V_x , and the density N of each data define a point in the V_x-N plane, marked by a circlet. The data are from the KH period (see the text related to Fig.1); the -177 km/s dotted line marks the V_x average. The radius of the small circlets is proportional to the data temperature (larger size corresponds to higher temperature). In addition, to help visibility, we

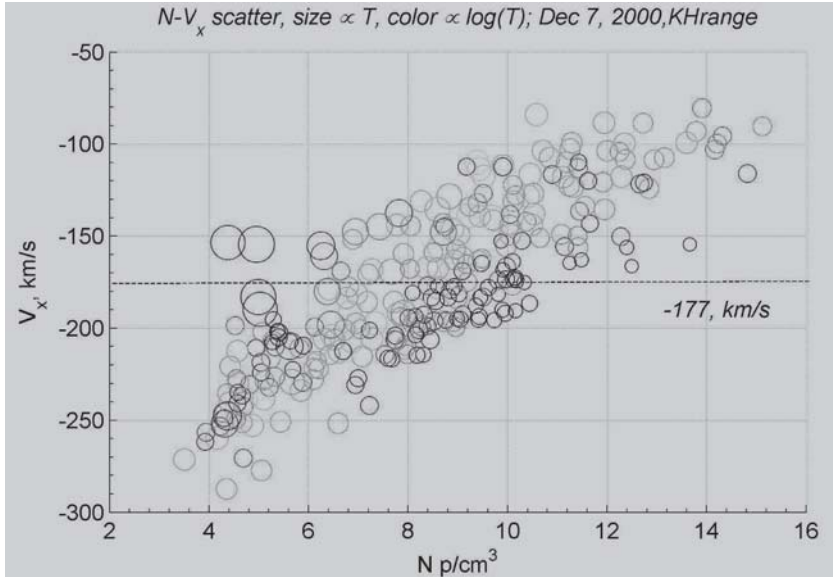


Figure 9. Scatter plot of December 7, 2000 V_x , versus N (data of the KH period). The size of the circlets is proportional to T , the intensity of gray proportional to $\ln(T)$ (lighter for high T).

set the gray scale of the marker proportional to $\ln(T)$ (lighter gray for hot matter, dark gray for cold matter). A logarithm scale is used because of the large range of temperatures displayed in the data.

A linear correlation exists, the majority of low-density plasma moves tailward, and the greater part of high density matter moves sunward. Some tenuous-hot data have very large anti-sunward speeds, and conversely some dense-cold plasma is moving very fast toward the sun.

A scatter plot of temperature, T , versus density, N , is shown in Figure 10. The size of the circlets is proportional to $|U_x|$, the absolute value of U_x , i.e., the tailward speed above the average. The circlets' gray shading indicates the sign of U_x , light gray is for sunward, and dark gray for tailward motion. The plot complements the correlation of Figure 9, showing at a glance that a large majority of dense plasma is in motion toward the sun, while on the other hand the greater part of tenuous matter moves anti-sunward. The size shows that there are fast members in both populations. There is a trend from higher to lower temperatures as we shift from lower to higher densities.

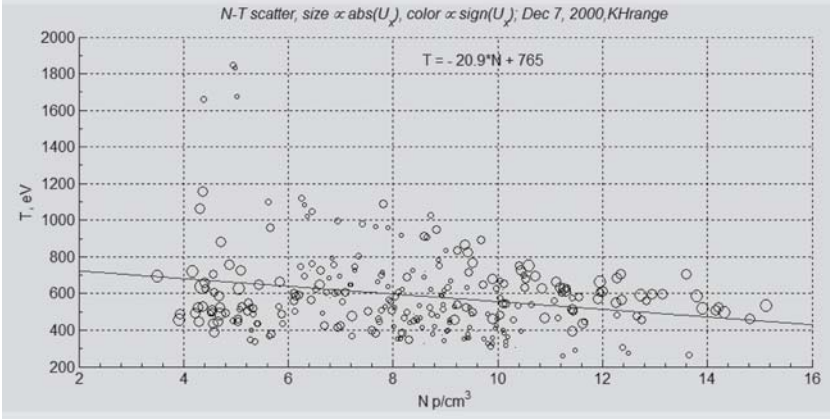


Figure 10. Scatter plot of T versus N . The size of the circlets is proportional to $|U_x|$, the gray shade indicates the sign of U_x (light for sunward motion, dark otherwise).

Figure 11 is a scatter plot of U_y versus U_x (GSM velocity components with average subtracted) where the circlets' size is proportional to N^2 (to enhance the tenuous - dense difference), and the gray scale is proportional to $\ln(T)$ (light gray for high temperatures). The time interval is, as before, the period of KH activity, 14.167 - 14.467 UT decimal hours (14:20-14:28 UT), when the IMF turns north. The motion is relative to the average of the observed plasma velocity.

The plot shows a linear correlation between $U_x = V_x - V_{xav}$ and $U_y = V_y - V_{yav}$, such that high speed, sunward motions, are predominantly inward oriented (and for the greater part associated with cold-dense plasma). Conversely, fast tailward motions are mainly outward directed (and correspond predominantly to hot-tenuous matter).

The data average of the velocity is the bulk speed of the plasma that passes over the position of the stationary spacecraft (the orbital speed of the device is insignificant compared with that of the plasma). With the scatter plots, we have shown that high temperature and low-density plasma patches, characteristic of inner layers (close to the magnetosphere) are moving tailward with velocities much higher than the average speed, with increments above average of 50-55%. On the other hand, cold and high-density plasma, typical of outer strata (close to the magnetosheath), are observed to move sunward with speeds about 50% higher than the interval average.

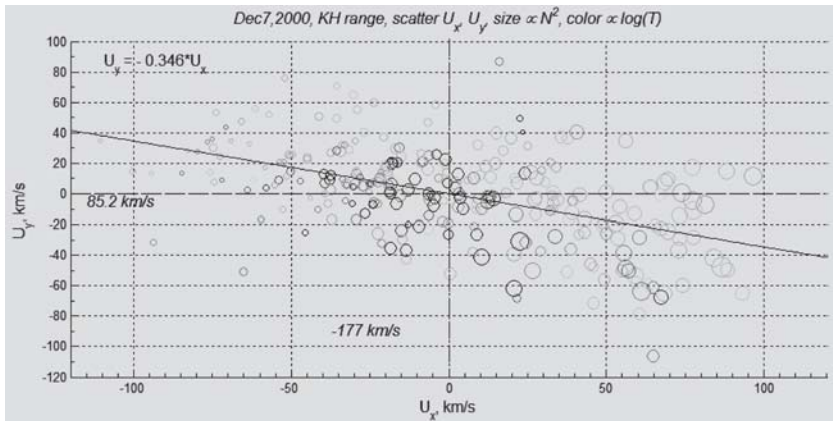


Figure 11. Scatter plot of December 7, 2000 data (KH period) U_y versus U_x . The circlets' size is proportional to N^2 , and the gray shade is proportional to $\ln(T)$ (lighter for high temperature).

Of course, there is also a large set of data with intermediate densities and temperatures, which are moving with velocities close to the bulk plasma speed. However, it is striking and we emphasize the fact, that large velocity differences with respect to the average, both in sunward and in tailward directions, are observed during the time lapse that is associated with the KH instability (because of the negligible magnetic shear). Moreover, we call the attention on the evidence that cold-dense plasma patches are moving sunward, against the magnetosheath flow, with speeds substantially larger than the recorded average, while fractions of tenuous-hot matter move tailward, also with velocities well in excess of the observed average.

Furthermore, because of the U_x - U_y linear correlation, the tailward accelerated hot-tenuous matter moves also predominantly outward (toward the magnetosheath). Conversely, the high speed cold-dense plasma moving sunward moves mostly inward (toward the magnetosphere). Thus, the scatter plots strongly suggest a composition of plasma motions, i.e., a rotational motion plus a bulk tailward translation, together with a rolling-over of plasma strata of different density and temperature. In other words, these are the trends qualitatively described by the LES reported in section 3, especially in subsection 3.5.

We consider the preceding set of correlations as embodying a criterion that allows, from records of one spacecraft alone, to decide

the presence of vortical motions in the BL, which therefore becomes an effective mixing layer of magnetospheric and magnetosheath plasmas.

5. Summary

The following is a summary of results reported in the paper.

- a. Deformation of the vorticity sheet and vortex division. Vorticity amplification by stretching, and frequency doubling.
- b. Generation of swirling flows (initially absent).
- c. Development of counter-rotating centers, with associations of positive – negative vorticity kernels.
- d. Presence of compressibility effects in the boundary layer, even for subsonic flows. In particular, the vortex core is affected in supersonic but not in subsonic flows.
- e. Magnetic “flutes” characterize the configuration; the vortex axis is along the magnetic field; LES show only moderate swaying of the magnetic lines.
- f. Evidence of magnetic strength enhancement around vortex kernels in supersonic flows, which is negligible at lower speeds.
- g. Mixing of magnetospheric and magnetosheath plasma; alternation of high-low density and low-high temperature strata.
- h. Formation of plasma hot spots, i.e., high temperature centers of low density.

The influence of increasing M and M_A was examined in all the points (a) to (h). In addition, guided by these results, and (g) in particular, as basic interpretive concepts, we examined scatter plots of velocity, density, and temperature of the event data to find signatures of the presence of vortices. As a consequence, we tested:

- i. A criterion to decide the presence of whirling plasma in the BL using records from one spacecraft alone.

Acknowledgements

Work supported by CONICET grant 11220090100608 PIP 2010 - 2012 (“*La Magnetopausa en Campo Magnético Interplanetario Norte: Análisis de Datos, Teoría y Simulación de Grandes Vórtices*”).

Work at University of New Hampshire was supported by NASA grant NNX08AD11G.

References

- [1] Gratton, F. T., *Anales Academia Nacional de Ciencias de Buenos Aires*, Tomo **XL**, pp. 57-80, 2007. ISBN 978-987-537-069-2
- [2] Gratton, F. T., Bilbao, L. E., Farrugia, C. J. and Gnani, G., 2009 *JOP Conf. Series* **166** 012023 doi:10.1088/1742-6596/166/1/012023
- [3] Gratton, F. T., *Anales de la Academia Nacional de Ciencias de Buenos Aires*, Tomo **XXXVI** (1), pp. 39-83, 2002. ISBN 987-537-030-4
Russel, C. T. and Kivelson, M. G. (eds.) 1995. *Introduction to Space Physics*, Cambridge Un. Press, New York.
- [4] Fairfield, D. H., Lepping, R. P., Hones, E. W., Bame, S. J. and Asbridge, J. R. 1981. *J. Geophys. Res.* **86** 1396.
- [5] Terasawa, T., *et al.* 1997 *Geophys. Res. Lett.* **24** 935.
Fujimoto, M. and Terasawa, T. 1994, *J. Geophys. Res.* **99** 8601.
- [6] Fujimoto, M., Mukai, T. and Kokubun, S. 2002 *Adv. Space Res.* **30** 2279.
- [7] Øieroset, M., *et al.* 2005 *Geophys. Res. Lett.* **32**, L12S07, doi:10.1029/2004GL021523.
- [8] Fujimoto, M., *et al.* 1998 *J. Geophys. Res.* **103** 4391.
- [9] Otto, A. and Fairfield, D. H. 2000 *J. Geophys. Res.* **105** 21175.
- [10] Fairfield, D. H., *et al.* 2000 *J. Geophys. Res.* **105** 21159.
- [11] Farrugia, C. J., Gratton, F. T. and Torbert, R. B. 2001 *Space Sci. Rev.* **95** 443.
- [12] Nykyri, K. and Otto, A. 2001 *Geophys. Res. Lett.* **28** 3565.
- [13] Otto, A. and Nykyri, K. 2003 *Geophys. Monogr.* **133** 53 eds. Newell, P. T. and Onsager, T. AGU Washington D.C.
- [14] Nakamura, T. K. M., Fujimoto, M. and Otto, A. 2006 *Geophys. Res. Lett.* **33** L14106 doi:10.1029/2006GL026318.
- [15] Nakamura, T. K. M., Fujimoto, M. and Otto, A. 2008 *J. Geophys. Res.* **113** A09204 doi:10.1029/2007JA012803.
- [16] Smets, R., Delcourt, D., Chanteur, G. and Moore, T. E. 2002 *Ann. Geophysicae* **20** 757.
- [17] Hasegawa, H., Fujimoto, M., Phan, T., *et al.* 2004 *Nature* **430**, 755.
- [18] Hasegawa, H., Fujimoto, M., Takagi, K., *et al.* 2006 *J. Geophys. Res.* **111** A09203 doi:10.1029/2006JA011728.
Takagi, K., Hashimoto, C., Hasegawa, H., Fujimoto, M., and TanDokoro, R., 2006, *J. Geophys. Res.*, **111**, A08202, doi:10.1029/2006JA011631.
- [19] Hasegawa, H., Retinò, A., Vaivads, A., *et al.* 2009 *J. Geophys. Res.* **114** A12207 doi: 10.1029/2009JA014042.
- [20] Gratton, F. T., Farrugia, C. J., Bilbao, L. E., Gnani, G. and Lund, E. 2006 *Am. Inst. of Physics C. P.* **875** Plasma and Fusion Science pp.300 - 303 ed. Herrera Vázquez J. J. E. Washington DC.

- [21] Gratton, F. T., Bender, L., Farrugia, C. J. and Gnani, G., 2004 *J. Geophys. Res.*, **109**, A04211, doi:10.1029/2003JA010146.
Gratton, F. T., Gnani, G., Farrugia, C. J., and Bender, L., 2004 *Brazilian J. of Physics*, **34**, 1804.
- [22] Le, G. and Russell, C. T. 1994 *Geophys. Res. Lett.* **21** 2451.
- [23] Farrugia, C. J., Gratton, F. T., Lund, E. J., *et al.* 2008 *J. Geophys. Res.* **113** A03208 doi:10.1029/2007JA012800.
- [24] Farrugia, C. J. and Gratton, F. T. 2009 *J. Atmos. Solar-Terr. Phys.* doi:10.1016/j.jastp.2009.10.008.
- [25] Foullon, C., Farrugia, C. J., Fazakerley, A. N., *et al.* 2008 *J. Geophys. Res.* **113** A11203 doi:10.1029/2008JA013175.
Foullon, C., Farrugia, C. J., Fazakerley, A. N., *et al.* 2010 *J. Geophys. Res.* **115** A09203 doi:10.1029/2009JA015189.
- [26] Gnani, G., Gratton, F. T., Farrugia, C. J. and Bilbao, L. E. 2009 *J. of Physics C.S.* **166**, 012022 doi:10.1088/1742-6596/166/1/012023.
- [27] Farrugia, C. J., Erkaev, N., Torbert, R., *et al.* 2010 *J. Geophys. Res.* **115** A08227 doi:10.1029/2009JA015128.
- [28] Bilbao, L. E. 1990 *J. Computational Physics*, **91**, 361.
- [29] Bilbao, L. E. and Linhart, G. 1996 *Plasma Physics Reports (Fizika Plazmy)* **22**, 457.
- [30] Linhart, G. and Bilbao, L. E. 2002, *IEEE Trans. Plasma Science*, **30** pp. 460-467.
- [31] Bilbao, L. E. 2006 *Am. Inst. of Physics C. P.* **875** *Plasma and Fusion Science* pp. 467-472.
- [32] Bilbao, L. E. 2009 *J. of Physics*, C.S. **166** 012020 doi:10.1088/1742-6596/166/1/012020.
- [33] Lesieur, M., 1990 *Turbulence in Fluids*, Kluwer Academic Pub., Dordrecht.